TiO2 and activated carbon of Argania Spinosa tree nutshells composites for the adsorption photocatalysis removal of pharmaceuticals from aqueous solution

El Mountassir El Mouchtari, Claude Daou, Salah Rafqah, Fadia Najjar, Hafid Anane, Anne Piram, Aline Hamade, Samir Briche, Pascal Wong-Wah-Chung

TiO_2 and activated carbon of *Argania Spinosa* tree nutshells composites for the adsorption photocatalysis removal of pharmaceuticals from aqueous solution

El Mountassir El Mouchtari [1,2], Claude Daou [3], Salah Rafqah[1], Fadia Najjar [3], Hafid Anane [1], Anne Piram [2], Aline Hamadeh [3], Samir Briche [4], Pascal Wong-Wah-Chung* [2].

[1] LCAM, Faculté Polydisciplinaire de Safi, Université Cadi Ayyad, Morocco
[2] Aix Marseille Univ, CNRS, LCE, Marseille, France
[3] Université Libanaise, Faculté des Sciences II, Fanar, Lebanon
[4] Département stockage de l'énergie et revêtements multifonctionnels, MAScIR, Rabat, Morocco

* Corresponding authors:

Pascal Wong-Wah-Chung: Université Aix-Marseille -Laboratoire de Chimie de l'Environnement-UMR CNRS 7376-Europôle de l'Arbois -Bât Villemin – BP80 – 13545 Aix-en-Provence Cedex 4, France

pascal.wong-wah-chung@univ-amu.fr

Tel.; +33 4 42 90 84 16

"In Memory of the Late Professor Moulay Lahcen EL IDRISSI MOUBTASSIM, Everybody who knew him will forever remember this brilliant scientist and true gentleman".

Abstract: This work demonstrates the interest of new bio composite materials for the elimination of pharmaceuticals (diclofenac (DCF), carbamazepine (CBZ) and sulfamethoxazole (SMX)) from aqueous solution. The synthesized materials are based on activated carbon (ACP) of *Argania Spinosa* tree nutshells by calcination and H_3PO_4 activation, and commercial TiO_2 (Degussa P25). AC/TiO_2 composite materials were prepared by temperature impregnation with different TiO_2 mass ratio (9, 16.6 and 33.3%). Characterization of AC and AC/TiO_2 revealed remarkable adsorption properties of bio sourced AC (BET surface area of 1159 m^2/g) and successful deposition of layer of TiO_2 on AC surface in controlled amount, with some physical changes (surface area and total pore volume decrease). Langmuir model describes efficiently adsorption of pharmaceuticals onto AC/TiO_2 with maximum capacities of 153.8, 105.3 and 125.0 mg/g at 25°C with 9% of TiO_2 (AC/TiO_2-9%) for DCF, CBZ and SMX, respectively. Photocatalytic activities of all composites were validated on CBZ. The elimination efficiency of relative high concentration of pharmaceuticals (50 mg/L) were proved with disappearances in the range of 50-100% after six hours upon simulated solar irradiation with the most interesting material AC/TiO_2-9% at a concentration of 0.1 g/L.

Keywords: *Argania Spinosa* tree nutshells, Activated carbon, TiO_2, Adsorption, Photocatalysis, Pharmaceuticals.

1. Introduction

In recent years, pharmaceutical products (PPs) used as human and veterinary drugs have been recognized as a health hazard for human health and have been impacting the ecosystem as well. Wastewater produced by pharmaceutical industries contains non-biodegradable organics, such as antibiotics drugs, ineffectively removed by traditional wastewater treatment systems [1,2]. Thus, some pharmaceutical by products end up as persistent contaminants in water bodies. They have been detected at concentrations between ng/L to g/L [3,4]. Among others, diclofenac (DCF), sulfamethoxazole (SMX) and carbamazepine (CBZ) are of great concern. DCF is a non-steroidal anti-inflammatory drug widely used to reduce inflammation and to relieve pain. Its annual worldwide consumption is estimated to be 940 tons per year in 2007 [5]. It has been detected at concentration up to 1.6 µg/L in wastewater treatment plants effluent where its removal efficiency varies in the range of 21-40% [6]. The effect of DCF on aquatic life has been evaluated and the results showed that DCF poses a risk to the ecosystems where it is present [7]. Sulfamethoxazole belongs to the sulfonamide class of antibacterial compounds, which is extensively used in veterinary and human medicine to treat respiratory, urinal, and gastrointestinal diseases [8]. SMX has been also detected in surface waters at levels between 30 to 480 ng/L [9]. The continuous exposure of bacteria to trace levels of antibiotics such as SMX in the aquatic environment can result in change of antibacterial genes and allows it to be more resistant to drugs [10]. Carbamazepine is a medicine prescribed to fight against partial epilepsies (brain reactions due to localized lesion) with abnormal movements (tonic-clonic) as well as to relieve some pains (facial neuralgia, painful neuropathies of patients of diabetics disorder). It has been detected at elevated concentration up to 6.3 µg/L in wastewater [11], also in surface waters at a concentration of 3.1 µg/L and in drinking water up to 43 ng/L [12].

To overcome the discharge of pharmaceuticals in environmental compartments, various treatment techniques and processes have been used. Among them, advanced oxidation processes (AOPs): it has been proved morea efficient in many technologies for applications for treatment of toxic wastewater and non-biodegradable organics [13]. The most broadly adopted AOP is heterogeneous photocatalysis that uses TiO_2 as semiconductor. Because it is cheap, non-toxic, very active and stable in chemical reaction, it is widely adopted for water treatment [14–16]. However, there are some disadvantages to use TiO_2 in powder form in photocatalytic processes: difficulties to separate the powder from water, aggregation of the suspended powder of TiO_2 particularly at high concentrations [17,18]. Therefore, much attention has been paid for the development of alternative approach with TiO_2 deposited on a support with a high surface area [19]. Hence, different types of support for TiO_2 have been tested such a silica [20], perlite [21], zeolite [22], carbon black [23], and activated carbon [24]. Activated carbon has no photocatalytic activity but increases removal because of its strong adsorption capacity. Thus, it allows the transfer rate improvement of the interfacial charge and the decrease of the positive hole and electron recombination [25].

The objective of this work is to demonstrate the relevance of heterogeneous photocatalysis for the degradation of bio-recalcitrant pharmaceuticals with a new composite material. Herein, the synthesis pathway is described as well as the characterization of the material. In addition, kinetic studies were carried out to estimate the efficiency of the composites for the removal of pharmaceutical products by dual adsorption and photocatalysis capabilities.

2. Material and Methods

2.1. Chemicals

Carbamazepine (99% purity), diclofenac (98% purity), and sulfamethoxazole (98% purity) were purchased from Sigma-Aldrich (St-Louis, USA), and acetonitrile (HPLC grade) was provided by VWR chemicals (Fontenay-sous-Bois, France). Water and acetonitrile (Optima® LC/MS grade) were obtained from Fischer Scientific SAS (Fair Lawn, USA, and Geel, Belgium, respectively) and formic acid (LC/MS grade) was purchased from VWR chemical (Fontenay-sous-Bois, France). TiO_2 Degussa P25 was 80:20 Anatase: rutile with a surface area of 55 m^2/g. The activating chemical used was phosphoric acid (85%) purchased from Sigma Aldrich, and hydrochloric acid (37%) was provided from Sigma-Aldrich.

Aqueous CBZ, DCF and SMX solutions were prepared with a concentration equal to 50 mg/L with ultra-pure water from a Millipore device (Direct-Q® 5 UV) after 12h stirring at room temperature (25°C).

2.2. Synthesis of AC and AC-TiO_2

Activated carbon (AC) was prepared from Argan tree nutshells. They were repeatedly washed many times with distilled water, let to dry in the oven at 120°C for 60 min. These shells were crushed, powdered to small texture by ball milling using a planetary mill equipped of ZrO_2 balls. The particles size between 1 and 2 mm was selected using the sieve, immersed in a phosphoric acid solution (50% by weight/volume) and mixed (400 rpm) during 15 min. The mixture obtained was then dried in an oven overnight at 105°C.

The heating rate of carbonization was programmed at $5°C.min^{-1}$ in the muffle furnace under atmospheric conditions without fresh air regeneration. It maintains until the final temperature of 500°C was reached and it was kept at this temperature for 60 min. After cooling, the black carbonaceous residue obtained was washed five times with HCl (0.1 M) and repeatedly washed with distilled water to neutralize the pH. The product washed was dried at 120°C for 10 hours, then crushed until a fine powder (AC) was obtained.

The preparation of the composite was undertaken by applying to the high-temperature impregnation method described by El-sheikh et al. [26]. Thus, a variable mass of TiO_2 Degussa P25 (0.1; 0.2 and 0.5 g) was stirred and heated in 50 mL of distilled water at 70°C. One gram of AC was added, and the stirring took place continuously for 60 min to allow the disappearance of the black AC and white TiO_2 particles phases to give a final unique grey-colored phase. The supernatant was decanted and the solid was dried at 150°C for 3h. The solid was then washed three times with distilled water to remove non-interacted TiO_2, and then dried again at 150°C for 10h.

2.3. Characterization of AC and AC/TiO_2

FTIR spectra were conducted on a THERMO ELECTRON corporation spectrometer (Nicolet NEXUS FT-IR), using KBr pellets for sample preparation. The morphology and structure of the sample were observed by high-resolution scanning electron microscopy (SEM) using BRUKER-QUANTAX FEI instrument operated at 200 keV, equipped with an energy dispersive spectrometer (EDS). Thermogravimetric analysis (TGA) was performed in Air atmosphere using TGA Q500 (TA 1000) equipment. The specimens (approximately 20 mg) were weight in Platinum crucible. The samples were heated at a rate of 5°C/min from ambient temperature to

1000°C. X-ray diffraction (XRD) measurements were performed by a BRUKER-D8 Advance diffractometer using Cu Kα X-ray source (λ = 0.15418 nm) as an incident radiation. The specific surface area of samples was measured using a Micromeritics 3-FLEX and the Brunauer-Emmett-Teller (BET) method at 77K with nitrogen adsorption and desorption.

2.4. Photocatalysis experiments

Irradiation was realized using a LOT Quantum Design Xenon lamp system (300 W) equipped with a 90° beam turner whose emission was filtrated by a water and atmospheric filter (LOT Quantum Design LSZ231 and LSZ176) to deliver 290-800 nm wavelength [27]. 50 mL of the mixture was placed in a reactor, and the solution was continuously stirred along the experiment. Sample and reactor were kept at 20°C by a water flow.

2.5. HPLC analysis of PPs

The concentration of pharmaceuticals was determined by liquid chromatography apparatus (UPLC PerkinElmer Altus 30) equipped with a Eclipse Plus C18 (3,5 µm; 2,5 × 150 mm) and a 220/240 pump, a 330 diode array UV-visible detector, a 363 fluorescence detector and a 410 automatic injector. An isocratic method set at a flow rate of 0.25 mL/min for CBZ and SMX and 0.35 mL.min^{-1} for DCF. The injected volume was equal to 10 µL. The separation was obtained using a mixture of water/acetonitrile (with 0.1% formic acid) ratio of 65:35 for the analysis of CBZ and SMX and a 50:50 ratio for the elution of DCF. The detection of pharmaceuticals was realized using 285, 275 and 268 nm absorption wavelength for CBZ, DCF and SMX, respectively. Before injection, samples were systematically filtered on a 0.2 µm cellulosic filter of 15 mm in diameter and the non-retention of pharmaceutical compounds on filters has been tested. The filter purchased by Agilent Technologies was used to remove the photocatalyst.

2.6. PPs adsorption equilibrium on composite materials

In order to evaluate the adsorption ability of the composite materials for CBZ, DCF and SMX adsorption experiment was carried out in dark condition at 25°C with a concentration of pharmaceutical equal to 50 mg/L and AC/TiO_2 at 0.1 g/L. All along the measurement (2 h), magnetic stirring was applied to reach the adsorption-desorption equilibrium. Sampling was realized at different time intervals and LC analyses allowed to determine the residual concentration of CBZ, SMX and DCF.

The adsorption capacity (q in mg g^{-1}) was calculated by using equation 1:

$$\boldsymbol{q = \frac{(C_0 - C_t)V}{m}} \qquad (5)$$

Where C_0 and C_t are the initial and final concentration (mg/L) of the pharmaceuticals in solution, respectively, V is the solution volume (L), and m is the mass (g) of AC/TiO_2.

3. Results and discussion

3.1. Characterization of AC and AC/TiO_2 composites

FTIR spectra of TiO_2, AC and AC/TiO_2 with a ratio TiO_2 versus AC equal to 9 % (AC/TiO_2-9%) are presented in Fig. 1. The large band at 3415 cm^{-1} is attributed to the OH stretching mode. These bands should

correspond to O-H vibration of the Ti-OH groups and H_2O molecules. The sharp band at 2912 and 2852 cm^{-1} are assigned to aliphatic C-H stretching. The peak observed at 1575 cm^{-1} characterized the vibration of C=C band. The rather narrow bands around 1547 and 1400 cm^{-1} can be attributed to OH mode (bending mode) of hydroxyl (OH) groups. The broadband at 611 cm^{-1} describes the stretching of Ti-O bond which is characteristic of the formation of TiO_2 in the activated carbon [. Moreover, the disappearance of the small band located at 3690 cm^{-1}corresponding to free OH in the AC/TiO_2 composite spectrum confirms that the TiO_2 nanoparticles were bound intimately to the ACP networks.

Fig. 1. FTIR spectrum of pure TiO_2 Degussa P25, AC and AC/TiO_2-9%

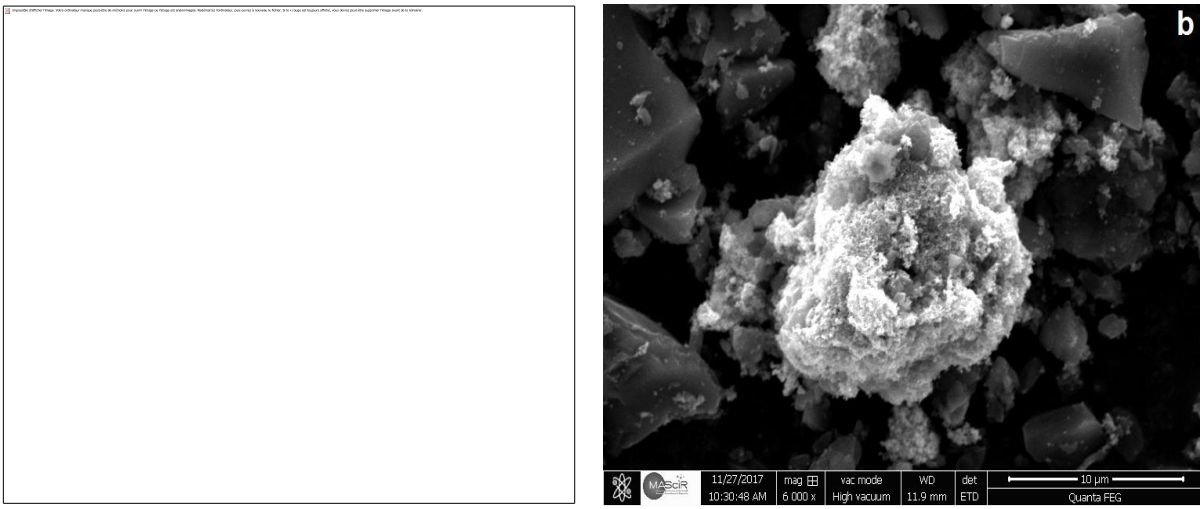

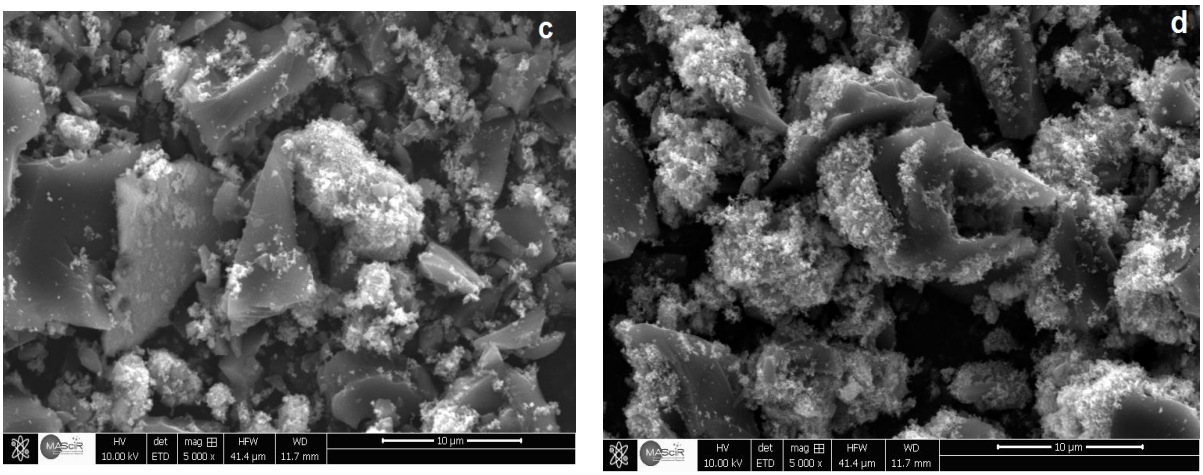

Fig. 2. SEM image of AC (a), AC/TiO_2: 9% (b), 16.6% (c) and 33% (d)

Fig. 2 illustrates the superficial morphology of AC with different content of TiO_2 (9, 16.6 and 33.3%) obtained by SEM experiments. The image (a) shows that the activated carbon particulates have irregular shapes. After deposition of different content of TiO_2, the formation of a layer on AC surface is observed. At higher TiO_2 content in AC/TiO_2 (Fig. 2c and 2d), it can be clearly seen that the supported TiO_2 particles which appear in light grey color, form aggregates and do not get homogeneously dispersed. EDX analysis indicates qualitatively the presence of TiO_2 on the surface of AC and other elements, such as C, P, O, and N which are constituents of the mineral composition of AC (EDX spectrum in Fig. S1).

Accurate TiO_2 mass in the synthesized composite was estimated by TGA experiments. The thermograms obtained for AC and AC/TiO_2 samples are shown in Fig. 3 with two major steps of weight loss. The first thermal event appears between 18.5 and 100°C with a comparable weight loss of 21.6% and 13.7 % for AC and AC/TiO_2-9%, respectively, probably due to the removal of adsorbed water from the activated carbon. The second step in the range 100 to 1000°C with a weight loss of 74.37 and 71.59 wt. % for ACP and AC/TiO_2-9%, respectively, corresponds mainly to the combustion of carbonaceous material. The uncomplete weight loss for AC/TiO_2 can be attributed to the presence of TiO_2 considering a residual mineral contribution in AC of 2%. Based on the previously exposed results, TiO_2 contents on the synthesized composites was calculated using the universal analysis 2000 Software and are gathered in Table 1. The results in Table 1 clearly show that the values correspond to the ones expected considering the synthesis pathway validating our approach for use low amount of titanium oxide

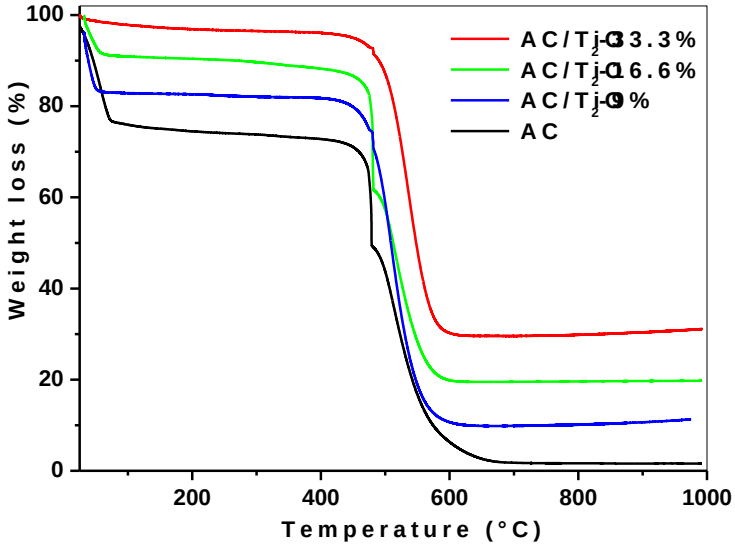

Fig. 3. TGA profile of AC and AC/TiO_2 composites

The synthesized composites AC/TiO_2 with different contents of TiO_2 and the raw materials TiO_2 and AC were also characterized by XRD technics. All XRD patterns are shown in Fig. 4. Two broad compressed peaks centered at 23.66° and 43.44° were characteristics of amorphous graphite of AC. These weak and undefined peaks indicate the low structural order of activated carbon. For TiO_2 Degussa P25, a sharp and strong peak at 2θ = 25.4° corresponding to the (101) plane of anatase structure of titanium is observed. Other less intense anatase peaks were also present in the XRD pattern at 2θ values of 36.9 (103), 37.7 (004), 38.5 (112), 48.0 (200), 53.9 (105), 55.0 (211), 62.6 (204), 68.9 (116), 70.2 (220) and 75.0° (215). Four other lower intensity peaks at 27.3, 36.0, 41.2 and 56.6° corresponding to the (110), (101), (111) and (220) planes are also evidenced and can be attributed to the rutile phase of Degussa P25 TiO_2. According to peak intensities, anatase phase is predominant relative to the rutile one as well-known for Degussa P25-TiO_2.

Fig. 4. XRD pattern of AC and AC/TiO_2 composites.

Based on the XRD result, the crystal size of the composite AC/TiO_2 was calculated using Scherrer's formula:

$$D = \frac{K*\lambda}{\beta\cos\theta} \qquad (1)$$

Where is the wavelength of the x-ray radiation (λ = 0.1541nm), k is Scherrer constant (k = 0.9), θ is the diffraction angle and β is the full-width-at-half-maximum of the (101) plane [28] The average size of crystallites of pure TiO_2-P25 and composite material AC/TiO_2 are listed in Table 1.

Table 1

TiO_2 content, crystallite size of TiO_2, surface area (S_{BET}), and total pore volume (TPV) of TiO_2, AC and AC/TiO_2 composites.

Sample	Calculated % TiO_2	Size(nm) TiO_2	S_{BET}(m^2/g)	TPV (cm^3/g)
TiO_2	/	22.1	55	/
AC	/	/	1159	0.64
AC/TiO_2 9%	9.28	24.2	959	0.52
AC/TiO_2 16.6%	17.7	22.7	948	0.54
AC/TiO_2 33.3%	29.2	23.4	859	0.48

These values put in evidence that the particle size of the photocatalyst in the AC/TiO_2 composite materials is almost comparable to the one of the commercial Degussa P25 anatase TiO_2. Because the very low temperature of composites preparation does not favor particle growth. The nitrogen adsorption-desorption isotherms for activated carbon and AC/TiO_2 composites with different TiO_2 percentage were recorded (see Fig. S2 for AC/TiO_2-9%in SI). The specific surface area was determined by using BET method and the results are gathered in Table 1. The BET specific surface area of activated carbon obtained from *Argania Spinosa* tree nutshells is of great interest with a value in the medium range of others surface areas of AC obtained with natural sources and calcination under nitrogen, such as *Cyclamen persicum* tubers (423.3-606.78 m^2/g), peach stones (1053 m^2/g), date stones (1044 m^2/g), coconut shells (850.64 m^2/g) or *Ziziphus spina-christi* seeds (914.23 m^2/g) [29-33].

The impregnation of TiO_2 on AC decreased the surface area and porous volume of AC/TiO_2 with a maximum of around 20% for the higher content in TiO_2. Such decrease of the surface area and pore volume has been previously observed with other bio composites [31,32]. As the percentage of TiO_2 increased, the surface area decreased as well as the pore volume. The pore volume associated to the small pores (below 3 nm) is particularly affected by the presence of TiO_2, even if the particle size of TiO_2 is more than 7 times higher (see Fig. S3. in SI). This is consistent with a deposition on the surface of AC and not directly inside the pores.

3.2 Adsorption equilibrium and kinetic studies

The kinetic adsorption study of carbamazepine and diclofenac showed similar behavior on the surface of active coal (AC). They reach equilibrium after 60 minutes of contact with an adsorption rate of about 70±1%. However, Sulfamethoxazole reached a plateau of 58% at the same time of contact. (see Fig. S4 in SI). With this approach, the adsorption efficiency of the composites (AC/TiO_2) was evaluated on CBZ used as a reference. The kinetics presented in Fig. 5 show two distinctive steps. A CBZ efficient adsorption takes place in the early stages of the experiments and an equilibrium sorption state is reached after around 60 min under stirring and at room temperature.

The maximum of CBZ adsorption around 50% is observed with the composite containing the lowest quantity of TiO_2 (AC/TiO_2-9%), in agreement with its highest specific area and pore total volume. Therefore, and considering that the adsorption efficiency should control the photocatalytic activity of the material as previously demonstrated, we focused our attention on AC/TiO_2-9% composite during the following set of experiments.

To better understand PPs adsorption mechanism on the surface of the materials, two widely used mathematical models for adsorption, Langmuir and Freundlich model, were investigated. These models related non-linearized expressions are expressed by equation 2 and 3, respectively [34:

$$qe = \frac{q_m K_L C_e}{1+K_L C_e} \qquad (2)$$

$$qe = K_f C_e^{1/n} \qquad (3)$$

Where q_e is the equilibrium amount of PP adsorbed per unit weight of the adsorbent (mg/g), q_m is the maximum adsorption capacity (mg/g), K_L is the intensity of adsorption (L/mg), Ce is the equilibrium concentration of PP (mg/L), K_f is relative adsorption capacity ((mg/g) $(mg/L)^{-n}$) and n are Freundlich isotherm constant.

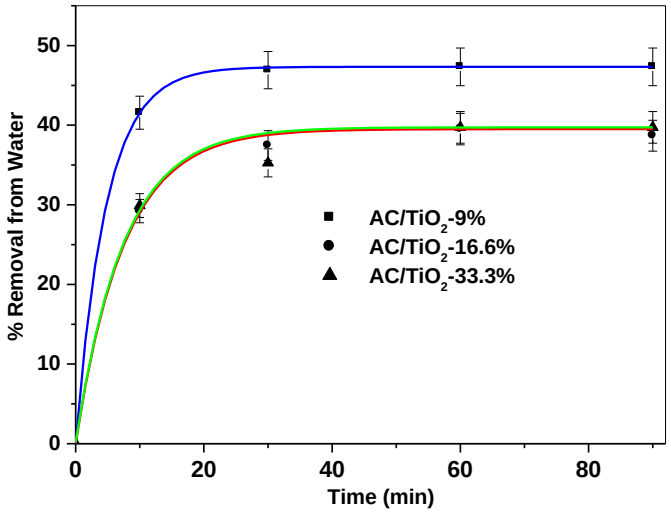

Fig. 5. Adsorption kinetics of CBZ on AC/TiO_2 composites in water: 9% (▲), 16.6% (■) and 33.3% (◆). [CBZ] = 50 mg/L, [composite] = 0.1 g/L, T = 25°C.

Experimental data of adsorption of CBZ on AC and AC/TiO_2 9% were fitted with Langmuir and Freundlich equations using OriginPro 8 SR0 OriginLab Corporation (Northampton, USA) as shown on Fig. 6 and for the other pharmaceuticals on Fig. S5. in SI. All parameter values and correlation coefficients for both isotherms are presented in table 2.

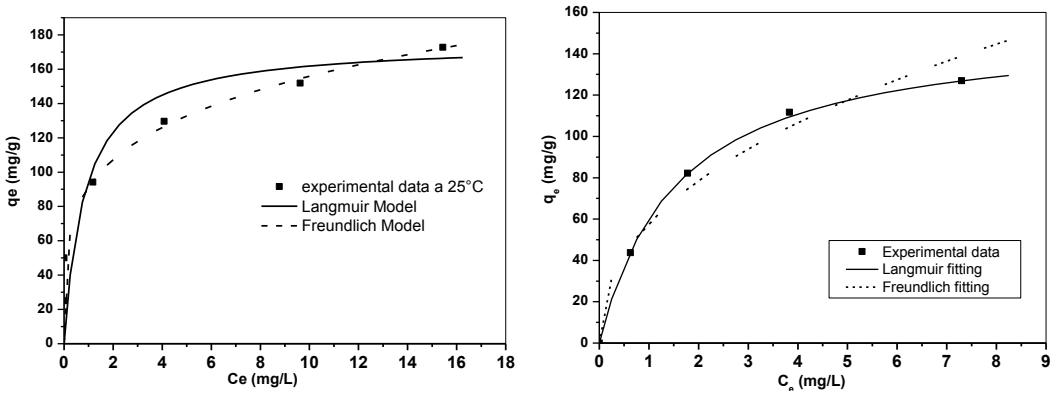

Fig. 6. Non-linear Langmuir and Freundlich isotherms obtained for CBZ adsorption on AC (left) and AC/TiO_2-9% (right). [CBZ] = 5 to 50 mg/L, [composite] = 0.1 g/L, T = 25°C.

According to the correlation coefficients (between 0.990 to 0.995), Freundlich model fits better with the multilayers adsorption of PPs on to AC [35] as previously described for DCF on Cyclamen persicum tubers based activated carbon [29] or for CBZ and SMX on other activated carbons K_f values in the range 51.6 to 71.4 (mg/g) $(mg/L)^{-n}$ reveals the great adsorption affinity of the pharmaceuticals with AC [36-37].

At the opposite, with R in the range 0.998 to 0.996, Langmuir model is considered more suitable to describe the mono-layer adsorption of all PPs onto AC/TiO_2 composite [38] probably because of presence of new adsorption sites such as Ti^{4+}. One can notice that Q_{max} values, in the range 105.3 to 153.8 mg/g, confirm the great adsorption affinity of the three pharmaceuticals for AC/TiO_2-9% composite without changing the affinity order observed with ACP: CBZ > SMX > DCF.

Table 2

Parameter values of PPs adsorption on AC and ACP/TiO_2 9% using Langmuir and Freundlich model, [PP] = 5 to 50 mg/L, [composite] = 0.1 g/L, T = 25°C.

Material	PP	Langmuir model			Freundlich model		
		Qmax (mg/g)	R	K_L (L/mg)	K_f (mg/g) $(mg/L)^{-n}$	R	1/n
AC/TiO_2 9%	**CBZ**	153.8	0.996	0.64	57.8	0.96	0.44
	DCF	105.3	0.988	0.87	17.1	0.95	0.267
	SMX	125.0	0.988	1.33	42.1	0.97	0.267
AC	**CBZ**	175.4	0.988	1.18	71.4	0.995	0.231
	DCF	121.9	0.98	0.29	51.6	0.99	0.237
	SMX	192.3	0.96	0.77	70.1	0.99	0.415

3.3 Photocatalytic studies

The photocatalytic activity of AC/TiO_2 composites was first evaluated with CBZ used as a model organic substrate for pharmaceuticals. This choice was made because CBZ was proved to be almost photostable in our experimental conditions as presented in Fig. S6 in SI.

The photodegradation of CBZ and other pharmaceuticals was carried out after stirring for 2 hours in the dark so that the adsorption/desorption equilibrium was attained (see Fig. S7 in SI). Even if CBZ adsorption has been

proved to be the most efficient with AC/TiO_2 9%, CBZ degradation kinetics were established with all materials in order to determine if an increase of TiO_2 percentage could affect the degradation rate of CBZ.

On the results illustrated in Fig. 7, it can be observed that the adsorption performance of AC/TiO_2-9% is confirmed and CBZ photoinduced degradation is very efficient and almost similar whatever the composite. However, it can be noticed that in the primary step of the degradation, the initial rates of CBZ transformation are slightly more important with low content of TiO_2 (rates equal to 0.137, 0.132 and 0.101 mg/L.min, respectively with TiO_2 content of 9, 16.6 and 33.3%). For longer irradiation time, the dissapearance of CBZ from the solution seems to be affected by the content in TiO_2 but without any well-defined tendency, probably resulting from secondary processes with photodegradation products of CBZ. Therefore, AC/TiO_2-9% biocomposite was chosen as a compromise issue due to its highest adsorption and degradation initial rate, and lowest production cost.

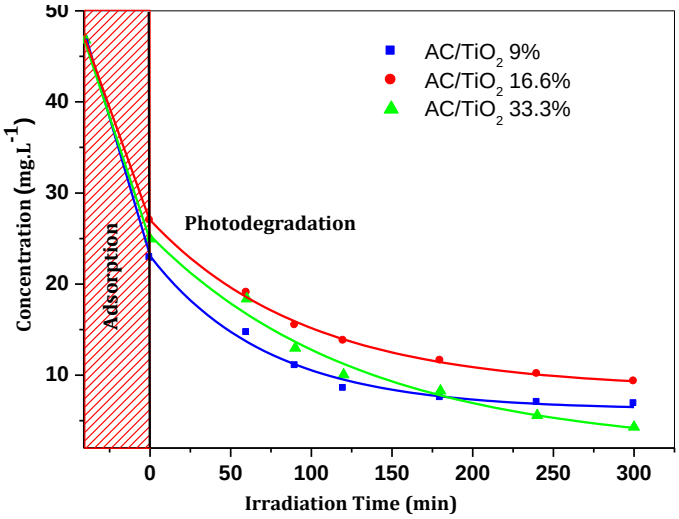

Fig. 7. CBZ degradation kinetics in the presence of different AC/TiO_2: 9% (●), 16.6% (▲) and 33.3% (■); [CBZ] = 50 mg/L, [AC/TiO_2] = 0.1 g/L, Xe lamp 300 W.

Before studying the photocatalytic efficiency of AC/TiO_2-9% on the other PPs, direct photolysis experiments were carried out on diclofenac and sulfamethoxazole. Thus, DCF and SMX degradation was observed with 68 and 14% of elimination, respectively, after 4h under irradiation, and initial rate equal to 0.222 and 0.092 mg/L.min (see Fig. S6 in SI).

In the presence of AC/TiO_2-9% and under irradiation, the degradation of the pharmaceuticals, presented in Fig. 8, occurs with various efficiency after the equilibrium sorption step. During the preliminary step, 48.9, 40 and 54% of CBZ, DCF and SMX are respectively adsorbed on AC/TiO_2-9%. After this step, the exposure leads to the fast disappearance of the pharmaceuticals with initial rates equal to 0.327, 0.715 and 0.185 mg/L.min for CBZ, DCF and SMX, respectively. In addition, after 4h of exposure, 100% of remaining DCF have disappeared from the solution and 50% of remaining SMX and 70% of remaining CBZ. In addition, this photodegradation, in terms of rate constant varied from one pollutant to another following the pseudo first order kinetic (Fig. 8-b).

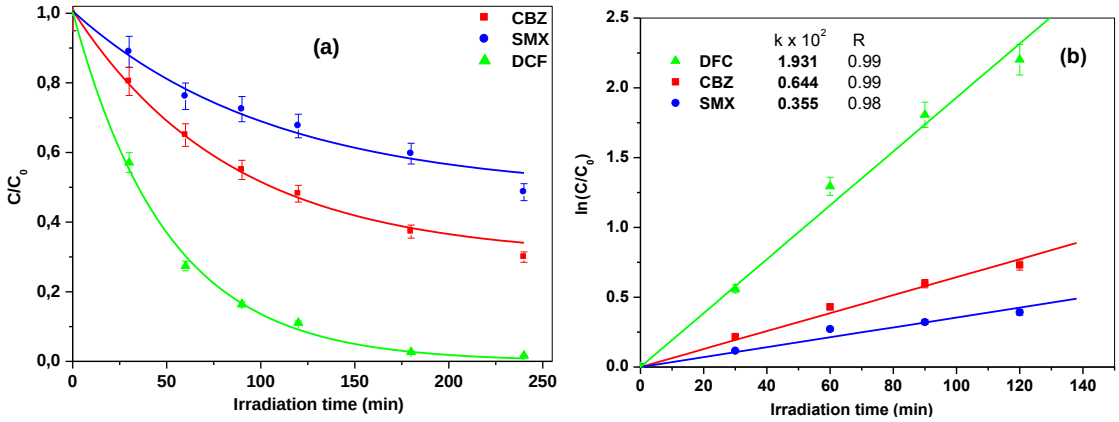

Fig. 8. Kinetics of the photodegradation (a) and kinetic model (b) in the presence of AC/TiO_2-9%: CBZ (■), DCF (▲) and SMX (●). [PP] = 50 mg/L, [AC/TiO_2-9%] = 0.1 g/L, Xe lamp 300 W.

In our experimental conditions, the remaining DCF disappearance under irradiation in the presence of the biocomposite could be mainly attributed to its direct photolysis while for SMX both photolysis and photoinduced transformation processes are implied and exclusively photoinduced process for CBZ.

Thus, for CBZ and SMX, the presence of TiO_2 deposited on the porous surface of activated carbon unambiguously improves their removal in the aqueous phase by the photoinduced chemical pathway. Such reactivity is attributed to the large surface area and ability of AC to adsorb the pollutant and bring it closer to the surface of TiO_2 particles, which increases the photocatalytic of TiO_2 because of its transfer rate improvement of the interfacial charge and the decrease of the positive hole and electron recombination **[24].**

In the presence of AC/TiO_2-9% composite, the adsorption-photodegradation processes implied in the removal of PPs from the solution lead to the removal of 85, 100, and 67% of CBZ, DCF and SMX, respectively, after 4 h of exposure. Even if previous works on biocomposites demonstrated the removal of CBZ, DCF and SMX by adsorption and photocatalysis **[39-41**, AC/TiO_2-9% composite allows more efficient elimination with low catalyst loading (0.1 g/L), high PP concentration (50 mg/L), and a reasonable time scale of a few hours.

4. Conclusions

Activated carbon was successfully prepared from *Argania Spinosa* tree nuts hells by calcination and acid activation as well as AC/TiO_2 composites by impregnation method with well-defined TiO_2 content. AC and AC/TiO_2 revealed to be very interesting and performing adsorption materials for diclofenac, carbamazepine and sulfamethoxazole. AC/TiO_2 composite showed a very great efficiency in the removal of the three pharmaceuticals from the solution by combining adsorption and photodegradation process, making this material as a promising and economically sustainable solution to water depollution.

5. Acknowledgments

The authors gratefully acknowledge the support by the Service de Coopération et d'Action Culturelle (SCAC) of the French Embassy and for funding this research through a PhD grant, for the CEDocs 2018 project, and the Francophone University Agency (AUF) is gratefully acknowledged.

Figure captions:

Fig. 1. FTIR spectrum of pure TiO_2 Degussa P25, AC and AC/TiO_2-9%

Fig. 2. SEM image of AC (a), AC/TiO_2: 9% (b), 16.6% (c) and 33% (d)

Fig. 3. TGA profile of AC and AC/TiO_2 composites

Fig. 4. XRD pattern of AC and AC/TiO_2 composites.

Fig. 5. Adsorption kinetics of CBZ on AC/TiO_2 composites in water: 9% (▲), 16.6% (■) and 33.3% (◆). [CBZ] = 50 mg/L, [composite] = 0.1 g/L, T = 25°C.

Fig. 6. Non-linear Langmuir and Freundlich isotherms obtained for CBZ adsorption on AC (left) and AC/TiO_2-9% (right). [CBZ] = 5 to 50 mg/L, [composite] = 0.1 g/L, T = 25°C.

Fig. 7. CBZ degradation kinetics in the presence of different AC/TiO_2: 9% (●), 16.6% (▲) and 33.3% (■); [CBZ] = 50 mg/L, [AC/TiO_2] = 0.1 g/L, Xe lamp 300 W.

Fig. 8. Kinetics of the photodegradation (a) and kinetic model (b) in the presence of AC/TiO_2-9%: CBZ (■), DCF (▲) and SMX (●), [PP] = 50 mg/L, [AC/TiO_2-9%] = 0.1 g/L, Xe lamp 300 W.

Table legends:

Table 1

TiO_2 content, crystallite size of TiO_2, surface area (S_{BET}), and total pore volume (TPV) of TiO_2, AC and AC/TiO_2 composites.

Table 2

Parameter values of PPs adsorption on AC and AC/TiO_2 9% using Langmuir and Freundlich model, [PP] = 5 to 50 mg/L, [composite] = 0.1 g/L, T = 25°C.

References

[1] J. Li, Z. Jin, Effect of hypersaline aniline-containing pharmaceutical wastewater on the structure of activated sludge-derived bacterial community, J. Hazard. Mater. 172 (2009) 432–438. doi:10.1016/j.jhazmat.2009.07.031.

[2] T.A. Ternes, M. Meisenheimer, D. McDowell, F. Sacher, H.-J. Brauch, B. Haist-Gulde, G. Preuss, U. Wilme, N. Zulei-Seibert, Removal of Pharmaceuticals during Drinking Water Treatment, Environ. Sci. Technol. 36 (2002) 3855–3863. doi:10.1021/es015757k.

[3] W.-J. Sim, J.-W. Lee, J.-E. Oh, Occurrence and fate of pharmaceuticals in wastewater treatment plants and rivers in Korea, Environ. Pollut. 158 (2010) 1938–1947. doi:10.1016/j.envpol.2009.10.036.

[4] Q. Sui, X. Cao, S. Lu, W. Zhao, Z. Qiu, G. Yu, Occurrence, sources and fate of pharmaceuticals and personal care products in the groundwater: A review, Emerg. Contam. 1 (2015) 14–24. doi:10.1016/j.emcon.2015.07.001.

[5] Y. Zhang, S.-U. Geißen, C. Gal, Carbamazepine and diclofenac: Removal in wastewater treatment plants and occurrence in water bodies, Chemosphere. 73 (2008) 1151–1161. doi:10.1016/j.chemosphere.2008.07.086.

[6] Y. Luo, W. Guo, H.H. Ngo, L.D. Nghiem, F.I. Hai, J. Zhang, S. Liang, X.C. Wang, A review on the occurrence of micropollutants in the aquatic environment and their fate and removal during wastewater treatment, Sci. Total Environ. 473–474 (2014) 619–641. doi:10.1016/j.scitotenv.2013.12.065.

[7] J. Schwaiger, H. Ferling, U. Mallow, H. Wintermayr, R.D. Negele, Toxic effects of the non-steroidal anti-inflammatory drug diclofenac: Part I: histopathological alterations and bioaccumulation in rain bow trout, Aquat.Toxicol. 68 (2004) 141–150. doi:10.1016/j.aquatox.2004.03.014.

[8] S. Mookherjee, C. Shoen, M. Cynamon, In Vitro Activity of JPC 2067 Alone and in Combination with Sulfamethoxazole against Nocardia Species, Antimicrob Agents Chemother. 56 (2012) 1133–1134. doi:10.1128/AAC.05855-11.

[9] J. Niu, L. Zhang, Y. Li, J. Zhao, S. Lv, K. Xiao, Effects of environmental factors on sulfamethoxazole photodegradation under simulated sunlight irradiation: kinetics and mechanism, J Environ Sci (China). 25 (2013) 1098–1106.

[10] Y. Yang, X. Lu, J. Jiang, J. Ma, G. Liu, Y. Cao, W. Liu, J. Li, S. Pang, X. Kong, C. Luo, Degradation of sulfamethoxazole by UV, UV/H2O2 and UV/persulfate (PDS): Formation of oxidation products and effect of bicarbonate, Water Res. 118 (2017) 196–207. doi:10.1016/j.watres.2017.03.054.

[11] T.A. Ternes, Occurrence of drugs in German sewage treatment plants and rivers1Dedicated to Professor Dr. Klaus Haberer on the occasion of his 70th birthday.1, Water Res. 32 (1998) 3245–3260. doi:10.1016/S0043-1354(98)00099-2.

[12] A. Togola, H. Budzinski, Multi-residue analysis of pharmaceutical compounds in aqueous samples, J.Chromatogr. A. 1177 (2008) 150–158. doi:10.1016/j.chroma.2007.10.105.

[13] J.C. Garcia, J.L. Oliveira, A.E.C. Silva, C.C. Oliveira, J. Nozaki, N.E. de Souza, Comparative study of the degradation of real textile effluents by photocatalytic reactions involving UV/TiO_2/H_2O_2 and UV/Fe^{2+}/H_2O_2 systems, J. Hazard. Mater. 147 (2007) 105–110. doi:10.1016/j.jhazmat.2006.12.053.

[14] S. Helali, E. Puzenat, N. Perol, M.-J. Safi, C. Guillard, Methylamine and dimethylamine photocatalytic degradation—Adsorption isotherms and kinetics, Applied Catalysis A: General. 402 (2011) 201–207. doi:10.1016/j.apcata.2011.06.004.

[15] A.A. Vega, G.E. Imoberdorf, M. Mohseni, Photocatalytic degradation of 2,4-dichlorophenoxyacetic acid in a fluidized bed photoreactor with composite template-free TiO_2 photocatalyst, Appl. Catal. A Gen 405 (2011) 120–128. doi:10.1016/j.apcata.2011.07.033.

[16] S. Rafqah, P. Wong-Wah-Chung, S. Nelieu, J. Einhorn, M. Sarakha, Phototransformation of triclosan in the presence of TiO_2 in aqueous suspension: Mechanistic approach, Appl. catal B : Enviro. 66 (2006) 119–125. doi:10.1016/j.apcatb.2006.03.004.

[17] P. Fernández-Ibáñez, J. Blanco, S. Malato, F.J. de las Nieves, Application of the colloidal stability of TiO2 particles for recovery and reuse in solar photocatalysis, Water Res. 37 (2003) 3180–3188. doi:10.1016/S0043-1354(03)00157-X.

[18] R. Molinari, M. Mungari, E. Drioli, A. Di Paola, V. Loddo, L. Palmisano, M. Schiavello, Study on a photocatalytic membrane reactor for water purification, Catal. Today. 55 (2000) 71–78. doi:10.1016/S0920-5861(99)00227-8.

[19] D.S. Bhatkhande, V.G. Pangarkar, A.A.C.M. Beenackers, Photocatalytic degradation for environmental applications – a review, J. Chem. Technol. Biotechnol. 77 (2002) 102–116. doi:10.1002/jctb.532.

[20] R. van Grieken, J. Aguado, M.J. López-Muñoz, J. Marugán, Synthesis of size-controlled silica-supported TiO_2 photocatalysts, J. Photochem. Photobiol. Chem. 148 (2002) 315–322. doi:10.1016/S1010-6030(02)00058-8.

[21] S.N. Hosseini, S.M. Borghei, M. Vossoughi, N. Taghavinia, Immobilization of TiO_2 on perlite granules for photocatalytic degradation of phenol, Appl. Catal. B Environ. 74 (2007) 53–62. doi:10.1016/j.apcatb.2006.12.015.

[22] T. Hisanaga, K. Tanaka, Photocatalytic degradation of benzene on zeolite-incorporated TiO_2 film, J. Hazard. Mater. 93 (2002) 331–337. doi:10.1016/S0304-3894(02)00050-X.

[23] A. Jitianu, T. Cacciaguerra, R. Benoit, S. Delpeux, F. Béguin, S. Bonnamy, Synthesis and characterization of carbon nanotubes–TiO_2 nanocomposites, Carbon. 42 (2004) 1147–1151. doi:10.1016/j.carbon.2003.12.041.

[24] E. Carpio, P. Zúñiga, S. Ponce, J. Solis, J. Rodriguez, W. Estrada, Photocatalytic degradation of phenol using TiO_2 nanocrystals supported on activated carbon, J. Mol. Catal. Chem. 228 (2005) 293–298. doi:10.1016/j.molcata.2004.09.066.

[25] T.-T. Lim, P.-S. Yap, M. Srinivasan, A.G. Fane, TiO2/AC Composites for Synergistic Adsorption-Photocatalysis Processes: Present Challenges and Further Developments for Water Treatment and Reclamation, Crit. Rev. Environ. Sci. Technol. 41 (2011) 1173–1230. doi:10.1080/10643380903488664.

[26] A.H. El-Sheikh, A.P. Newman, H. Al-Daffaee, S. Phull, N. Cresswell, S. York, Deposition of anatase on the surface of activated carbon, Surf. Coat. Technol. 187 (2004) 284–292. doi:10.1016/j.surfcoat.2004.03.012.

[27] R. Meribout, Y. Zuo, A.A. Khodja, A. Piram, S. Lebarillier, J. Cheng, C. Wang, P. Wong-Wah-Chung, Photocatalytic degradation of antiepileptic drug carbamazepine with bismuth oxychlorides (BiOCl and BiOCl/AgCl composite) in water: Efficiency evaluation and elucidation degradation pathways, J. Photochem. Photobiol. Chem. 328 (2016) 105–113. doi:10.1016/j.jphotochem.2016.04.024.

[28] Y. Xie, C. Yuan, Visible-light responsive cerium ion modified titania sol and nanocrystallites for X-3B dye photodegradation, Appl. Catal. B Environ. 46 (2003) 251–259. doi:10.1016/S0926-3373(03)00211-X.

[29] S. Jodeh, F. Abdelwahab, N. Jaradat, I. Warad, W. Jodeh, Adsorption of diclofenac from aqueous solution using *Cyclamen persicum* tubers based activated carbon (CTAC), J. Assoc. Arab Univ. Basic Appl. Sci. 20 (2016) 32–38. doi:10.1016/j.jaubas.2014.11.002.

[30] T.S. Jamil, M.Y. Ghaly, N.A. Fathy, T.A. Abd el-halim, L. Österlund, Enhancement of TiO_2 behavior on photocatalytic oxidation of MO dye using TiO_2/AC under visible irradiation and sunlight radiation, Sep. Purif. Technol. 98 (2012) 270–279. doi:10.1016/j.seppur.2012.06.018.

[31] A. Omri, M. Benzina, Influence of the origin of carbon support on the structure and properties of TiO_2 nanoparticles prepared by dip coating method, Arab. J. Chem. (2015). doi:10.1016/j.arabjc.2015.06.027.

[32] Y. Liu, S. Yang, J. Hong, C. Sun, Low-temperature preparation and microwave photocatalytic activity study of TiO_2-mounted activated carbon, J. Hazard. Mater. 142 (2007) 208–215. doi:10.1016/j.jhazmat.2006.08.020.

[33] A. Omri, M. Benzina, Characterization of activated carbon prepared from a new raw lignocellulosic material: ziziphus spina-christi seeds, . J. Soc. Chim. Tunis. 2012, 14, 175-18

[34] A. Bonilla-Petriciolet, D.I. Mendoza-Castillo, H.E. Reynel-Ávila, eds., Adsorption Processes for Water Treatment and Purification, Springer International Publishing, 2017. https://www.springer.com/gp/book/9783319581354 (accessed March 25, 2019).

[35] E.S. Dragan, A.I. Cocarta, M.V. Dinu, Facile fabrication of chitosan/poly(vinyl amine) composite beads with enhanced sorption of Cu^{2+}. Equilibrium, kinetics, and thermodynamics, . Chem. Eng. J. 255 (2014) 659–669. doi:10.1016/j.cej.2014.06.098.

[36] M. Turk Sekulic, N. Boskovic, A. Slavkovic, J. Garunovic, S. Kolakovic, S. Pap, Surface functionalised adsorbent for emerging pharmaceutical removal: Adsorption performance and mechanisms, Process Saf. Environ. Prot. 125 (2019) 50–63. doi:10.1016/j.psep.2019.03.007.

[37] V. Calisto, C.I.A. Ferreira, J.A.B.P. Oliveira, M. Otero, V.I. Esteves, Adsorptive removal of pharmaceuticals from water by commercial and waste-based carbons, J. Environ. Manage. 152 (2015) 83–90. doi:10.1016/j.jenvman.2015.01.019.

[38] X. Hu, J. Wang, Y. Liu, X. Li, G. Zeng, Z. Bao, X. Zeng, A. Chen, F. Long, Adsorption of chromium (VI) by ethylenediamine-modified cross-linked magnetic chitosan resin: Isotherms, kinetics and thermodynamics, J. Hazard. Mater. 185 (2011) 306–314. doi:10.1016/j.jhazmat.2010.09.034.

[39] M. Gar Alalm, A. Tawfik, S. Ookawara, Enhancement of photocatalytic activity of TiO_2 by immobilization on activated carbon for degradation of pharmaceuticals, J. Environ. Chem. Eng. 4 (2016) 1929–1937. doi:10.1016/j.jece.2016.03.023.

[40] A. Carabin, P. Drogui, D. Robert, Photo-degradation of carbamazepine using TiO_2 suspended photocatalysts, J. Taiwan Inst. Chem. Eng. 54 (2015) 109–117. doi:10.1016/j.jtice.2015.03.006.

[41] L. Lin, H. Wang, P. Xu, Immobilized TiO_2-reduced graphene oxide nanocomposites on optical fibers as high performance photocatalysts for degradation of pharmaceuticals, Chem. Eng. J. 310 (2017) 389–398. doi:10.1016/j.cej.2016.04.024.